Explicit symplectic integrator for *s*-dependent static magnetic field

Y. K. Wu*
Department of Physics, Duke University, Durham, North Carolina 27708-0319, USA

E. Forest
High Energy Accelerator Research Organization, 1-1 Oho, Tsukuba, Ibaraki 305-0810, Japan

D. S. Robin
Lawrence Berkeley National Laboratory, 1 Cyclotron Road, Berkeley, California 94720, USA
(Received 22 June 2003; published 13 October 2003)

This paper reports our recent work on explicit symplectic integration techniques for the charged particle motion in an *s*-dependent static magnetic field. Using the extended phase space, symplectic integrators can be developed for Hamiltonians with or without the paraxial approximation using either the space or time as an independent variable. This work extends the successful element-by-element tracking method for studying single-particle nonlinear dynamics to a set of *s*-dependent magnetic elements. Important applications of this work include the studies of the charged particle dynamics in a storage ring with various insertion devices, superconducting magnets, large aperture magnets with significant fringe fields, and solenoid magnets in the interaction region. Consequently, this work is expected to make an impact on design and optimal operation of existing and future light source rings and high energy physics accelerators.

DOI: 10.1103/PhysRevE.68.046502 PACS number(s): 29.20.Dh, 29.27.Bd, 42.15.Eq

I. INTRODUCTION

Symplectic integrators are a set of special numerical integration methods developed for Hamiltonian systems. Unlike more widely used Runge-Kutta algorithms which are nonsymplectic in general, symplectic integration methods allow numerical computations of the phase space vector at any time τ, $\{\vec{q}(\tau),\vec{p}(\tau)\}$, so that the transformation from the initial state $\{\vec{q}(0),\vec{p}(0)\}$ to the final state $\{\vec{q}(\tau),\vec{p}(\tau)\}$ is canonical. The early application of higher-order (order $\geqslant 2$) explicit symplectic integrators in accelerator physics was initiated by Ruth's work for the following Hamiltonian [1]:

$$H=T(\vec{p})+V(\vec{q}). \tag{1}$$

Applying the Lie map techniques, Neri [2] and Forest [3] rederived Ruth's integrator, and found that such integrators were universally applicable to any Lie group. Later, Yoshida developed a systematic method [4] to construct higher-order integrators from a lower-order one. This work reduced the search for high-order symplectic integrators to that for a second-order integrator. The further development by Forest and others extended Yoshida's technique to the implicit integration and multimap explicit integration [5] as well as for the time-dependent Hamiltonians in the extended phase space [6].

In the storage ring, symplectic integration provides an essential tool to study the long-term beam dynamics. Magnetic multipole elements, such as quadrupoles and sextupoles, are modeled using a so-called impulse boundary approximation, in which the magnetic field is assumed to be constant (s independent) within the effective boundary of the magnet and zero outside. Such a field model allows one to use a special vector potential with only s component, $\vec{A}=A_s(x,y)\hat{s}$ for the magnet. Consequently, the Hamiltonian can be reduced to a drift-kick combination of the Ruth type: $H=T(\vec{p})+V(\vec{q})$, where $T(\vec{p})$ represents a drift and $V(\vec{q})$ a kick. Explicit symplectic integrators for such Hamiltonians have been implemented since the late 1980s in a number of tracking codes. These tracking codes have been widely used to compute charged particle trajectories for a large number of turns without introducing artificial damping or antidamping. These tools have been successfully utilized in developing third generation light storage rings with a small emittance as well as high energy physics collider rings with a high luminosity.

However, these types of symplectic integrators fail to model general nonmultipole elements with *s*-dependent magnetic fields such as wiggler and undulator magnets with alternating field polarity since their Hamiltonians can no longer be split into drift and kick combinations. Instead, the Hamiltonian for *s*-dependent static magnetic fields takes the following form:

$$H=T(\vec{p}-\vec{a}(\vec{q},s))+V(\vec{q},s). \tag{2}$$

Symplectic element-by-element tracking for this type of Hamiltonian is made possible using an integration method presented in this paper.

It is worth mentioning the recent work to study magnetic fringe field effects in the large hadron collider (LHC) and small rings with large apertures by Berz and co-workers [7,8]. They studied single-particle dynamics by iterating a high-order one-turn Taylor map extracted using a differential algebraic technique. In spite of its efficiency, semianalytic techniques based on the map iteration may be limited in their use without being benchmarked by element-by-element

*Electronic address: wu@fel.duke.edu

tracking. In fact, Abell *et al.* [9] showed that there existed an optimal order of one-turn map which would most accurately reproduce the LHC dynamics as compared with direct tracking. This finding clearly demonstrates the need for symplectic tracking models for three-dimensional (3D) magnetic field elements.

In this paper, the mathematical problem is first stated in Sec. II, followed by a brief revisit of Yoshida's procedure to construct higher-order symplectic integrators (Sec. III). Section IV lays out our development of explicit integrators for 3D static magnetic fields with the paraxial approximation. In Sec. V, the integration technique is extended to the exact Hamiltonian. This integration method has been used to develop a general symplectic tracking program for wigglers. Using the wiggler integrator, the dynamics impact of OK4 (optical-klystron) free electron laser (FEL) wigglers has been studied for the Duke storage ring (Sec. VI).

II. THE PROBLEM

The goal of this paper is to find explicit symplectic integrators for the charged particle Hamiltonian with *s*-dependent static magnetic field. Such a field depending on all three coordinates can be described in the Cartesian coordinate system by a vector potential of the form $\vec{A}(\vec{r}) = A_x(\vec{r})\hat{x} + A_y(\vec{r})\hat{y} + A_z(\vec{r})\hat{z}$, and $\vec{r} = (x,y,z)$. The corresponding Hamiltonian is

$$H(x,p_x,y,p_y,\delta,l;z) = -\sqrt{(1+\delta)^2 - (p_x - a_x)^2 - (p_y - a_y)^2} - a_z, \tag{3}$$

where $p_{x,y} = P_{x,y}/P_0$ is the scaled transverse momenta, P_0 is the nominal mechanical momentum, $\delta = |\vec{P} - (q/c)\vec{A}|/P_0 - 1$ is the relative momentum deviation, l is the path length, and $a_{x,y,z}(x,y,z) = qA_{x,y,z}(x,y,z)/(P_0 c)$ is the scaled vector potential.

As a special case, symplectic integrators for the magnetic multipole Hamiltonian with the square root had been developed by choosing $a_x = a_y = 0$ [6]. Tracking codes implementing this type of integrators include TEAPOT [10] and PTC [11].

However, in general, such a Hamiltonian contains terms which mix the coordinate and momentum of the same canonical pairs, such as in $[p_{x,y} - a_{x,y}(x,y,z)]^2$. Therefore, symplectic integrators developed for Hamiltonians of the Ruth type are no longer applicable. This problem is particularly difficult for the above form of the exact Hamiltonian in which the mixed terms are grouped together in the square root.

In large rings, the paraxial approximation can be made for the charged particle motion, which reduces the Hamiltonian to the following form:

$$H(x,p_x,y,p_y,\delta,l;z) \approx -\delta + \frac{(p_x - a_x)^2}{2(1+\delta)} + \frac{(p_y - a_y)^2}{2(1+\delta)} - a_z. \tag{4}$$

While the mixing of the coordinate and momentum remains in this Hamiltonian, the mixed terms are now all quadratic in form. Each quadratic term in the Hamiltonian has been found to be exactly integrable. This leads to an explicit symplectic integration scheme for *s*-dependent magnetic field (see Sec. IV).

III. YOSHIDA'S PROCEDURE REVISITED

Let us consider a time-independent Hamiltonian $H(\vec{q},\vec{p})$, its Lie map from a time 0 to a time t can be symbolically written as

$$\mathcal{M}(t) = \exp(t:-H:). \tag{5}$$

Suppose that this unsolvable Hamiltonian can be split into N solvable parts, $H = H_1 + H_2 + \cdots + H_N$, then a second-order integrator can be constructed using a symmetrized Lie map product [5]:

$$\mathcal{N}_i(t) = \exp(t:-H_i:), \quad i = 1,\ldots,N$$

$$\mathcal{M}_2 = \mathcal{N}_1(t/2)\mathcal{N}_2(t/2)\cdots\mathcal{N}_N(t)\cdots\mathcal{N}_2(t/2)\mathcal{N}_1(t/2) = \mathcal{M}(t) + O(t^3). \tag{6}$$

Yoshida's method [4] allows one to systematically construct a higher-order integrator from a lower-order one. Suppose that there exists a $(2n)$th-order symplectic approximation $\mathcal{M}_{2n}$ which has the property of time reversibility, $\mathcal{M}_{2n}^{-1}(t) = \mathcal{M}_{2n}(-t)$, then $\mathcal{M}_{2n}(t)$ would only contain odd power terms of time t in its Lie exponent [6]. $\mathcal{M}_{2n}(t)$ is then readily written as

$$\mathcal{M}_{2n}(t) = \exp[:-tH + t^{2n+1}F_{2n+1} + O(t^{2n+3}):].$$

A $(2n+2)$th-order integrator can be constructed in the following way:

$$\begin{aligned}\mathcal{M}_{2n+2}(t) &= \mathcal{M}_{2n}(x_1 t)\mathcal{M}_{2n}(x_0 t)\mathcal{M}_{2n}(x_1 t)\\ &= \exp[:-t(2x_1 + x_0)H + t^{2n+1}(2x_1^{2n+1} + x_0^{2n+1})F_{2n+1} + O(t^{2n+3}):]\\ &= \exp[:-tH + O(t^{2n+3}):].\end{aligned}$$

The last step is realized if

$$x_0 + 2x_1 = 1, \quad x_0^{2n+1} + 2x_1^{2n+1} = 0.$$

One set of trivial real solution is

$$x_0 = -\frac{2^{1/(2n+1)}}{2 - 2^{1/(2n+1)}}, \quad x_1 = \frac{1}{2 - 2^{1/(2n+1)}}. \tag{7}$$

The above procedure of Yoshida provides a recipe for constructing higher even order symplectic integrators from a lower-order one. The task of developing higher-order symplectic integrators for *s*-dependent magnetic elements is then reduced to the development of the lowest even order, i.e., second-order, integrator.

It is worth pointing out that Yoshida's procedure does not always produce the most effective higher-order integrators.

On the other hand, symplectic integration methods have been actively studied by mathematicians since 1990s as part of geometric integration [12]. Published references on a wide range of research in this area are documented by the SYNODE project [13]. For example, McLachlan's work on designing effective high-order integration methods [14] can provide valuable insights on developing more efficient integrators for our problem. In particular, we would like to evaluate a class of more efficient higher-order integrators with positive step size proposed by Nadolski and Laskar [15].

IV. SYMPLECTIC INTEGRATORS WITH PARAXIAL APPROXIMATION

The development of approximate Lie maps for z-dependent Hamiltonian of Eq. (4) can be facilitated by extending the phase space to include (z,p_z) as the fourth canonical pair and σ as an independent variable with $d\sigma=dz$ [6]. The equivalent paraxial Hamiltonian in the extended phase space is given by

$$K(x,p_x,y,p_y,\delta,l,z,p_z;\sigma)\approx -\delta+\frac{(p_x-a_x)^2}{2(1+\delta)}+\frac{(p_y-a_y)^2}{2(1+\delta)} -a_z+p_z. \tag{8}$$

Since this Hamiltonian is σ independent, an exact Lie map for an integration step $\Delta\sigma$ can be written symbolically as

$$\mathcal{M}(\Delta\sigma)=\exp(-\Delta\sigma:K:). \tag{9}$$

To simplify our derivation, a gauge transformation is made to yield a simpler vector potential with $A_z=0$: $\vec{A}=A_x(x,y,z)\hat{x}+A_y(x,y,z)\hat{y}$. Now by splitting the Hamiltonian to several parts,

$$K=K_1+K_2+K_3$$

with

$$K_1=p_z-\delta,\quad K_2=\frac{(p_y-a_y)^2}{2(1+\delta)},\quad K_3=\frac{(p_x-a_x)^2}{2(1+\delta)}.$$

A second-order approximation for $\mathcal{M}$ is constructed as follows:

$$\begin{aligned}\mathcal{M}_2(\Delta\sigma)&=\exp\left(:-\frac{\Delta\sigma}{2}K_1:\right)\exp\left(:-\frac{\Delta\sigma}{2}K_2:\right)\\&\times\exp(:-\Delta\sigma K_3:)\exp\left(:-\frac{\Delta\sigma}{2}K_2:\right)\\&\times\exp\left(:-\frac{\Delta\sigma}{2}K_1:\right)\\&=\mathcal{M}(\Delta\sigma)+O((\Delta\sigma)^3).\end{aligned}$$

Apparently, K_1 is exactly solvable due to the separation of the coordinate and momentum belonging to the same canonical pairs while K_2 and K_3 containing (x,p_x) and (y,p_y), respectively, remain unsolved. However, using the generating function technique, it can be shown that K_2 and K_3 are also exactly solvable.

Let us consider the Lie map $\exp(:-\Delta\sigma K_3:)$. Noticing that K_3 contains only p_x but not p_y, a generating function is in order to transform $(p_x-a_x)^2$ to $(p_x^{\text{new}})^2$ using a set of new canonical variables. The explicit Lie map for this generating function is

$$\mathcal{A}_x=\exp\left(:-\int a_x(x,y,z)dx:\right),$$

$$\exp\left(:-\frac{\Delta\sigma(p_x-a_x)^2}{2(1+\delta)}:\right)=\mathcal{A}_x\exp\left(:-\frac{\Delta\sigma p_x^2}{2(1+\delta)}:\right)\mathcal{A}_x^{-1}.$$

This generating function Lie map transforms the phase space variables explicitly as follows:

$$\mathcal{A}_x\{x,y,z,\delta,l\}=\{x,y,z,\delta,l\},$$

$$\mathcal{A}_x p_x=p_x-a_x,\quad \mathcal{A}_x^{-1}p_x=p_x+a_x,$$

$$\mathcal{A}_x p_y=p_y-\int\frac{\partial a_x}{\partial y}dx,\quad \mathcal{A}_x^{-1}p_y=p_y+\int\frac{\partial a_x}{\partial y}dx,$$

$$\mathcal{A}_x p_z=p_z-\int\frac{\partial a_x}{\partial z}dx,\quad \mathcal{A}_x^{-1}p_z=p_z+\int\frac{\partial a_x}{\partial z}dx.$$

In addition, the Lie map $\exp(:-\Delta\sigma p_x^2/2(1+\delta):)$ functions as a drift:

$$\exp\left(:-\frac{\Delta\sigma p_x^2}{2(1+\delta)}:\right)\{y,z,\delta,p_x,p_y,p_z\}=\{y,z,\delta,p_x,p_y,p_z\},$$

$$\exp\left(:-\frac{\Delta\sigma p_x^2}{2(1+\delta)}:\right)x=x+\frac{p_x}{1+\delta}\Delta\sigma,$$

$$\exp\left(:-\frac{\Delta\sigma p_x^2}{2(1+\delta)}:\right)l=l+\frac{p_x^2}{2(1+\delta)^2}\Delta\sigma.$$

Likewise, the Lie map $\exp[:-(\Delta\sigma/2)K_2:]$ can be exactly evaluated using a generating function Lie map, $\mathcal{A}_y=\exp(:-\int a_y(x,y,z)dy:)$.

Finally, we have completed the development of an explicit second-order symplectic integrator for $\mathcal{M}$:

$$\begin{aligned}\mathcal{M}_2&=\exp\left(:-\frac{(p_z-\delta)\Delta\sigma}{2}:\right)\mathcal{A}_y\exp\left(:-\frac{p_y^2\Delta\sigma}{4(1+\delta)}:\right)\mathcal{A}_y^{-1}\\&\times\mathcal{A}_x\exp\left(:-\frac{p_x^2\Delta\sigma}{2(1+\delta)}:\right)\mathcal{A}_x^{-1}\\&\times\mathcal{A}_y\exp\left(:-\frac{p_y^2\Delta\sigma}{4(1+\delta)}:\right)\mathcal{A}_y^{-1}\exp\left(:-\frac{(p_z-\delta)\Delta\sigma}{2}:\right).\end{aligned} \tag{10}$$

It is worth pointing out that this type of second-order approximations for $\mathcal{M}$ is not unique. By choosing different magnetic field gauges for the vector potential, one can construct an infinite set of second-order Lie map approximations

for the same Hamiltonian. It is expected that a particular choice of the vector potential can result in a more efficient symplectic integrator.

V. EXTENSION TO EXACT HAMILTONIAN

The development of symplectic integrators for the exact Hamiltonian of a 3D magnetic field becomes important when the paraxial approximation is no longer valid. One such example is a dipole magnet with a small bending radius in a compact storage ring. The integrators based upon an exact Hamiltonian can also be used to benchmark those based upon approximate Hamiltonians.

The development of explicit integrators in Sec. IV depends on the quadratic nature of the Hamiltonian. Consequently, this technique cannot be directly applied to the square-root form of the exact Hamiltonian [Eq. (3)]. However, we recognize that an equivalent exact Hamiltonian in the quadratic form can be constructed using several methods. One of them starts from a quadratic Lagrangian.

The following invariant quadratic Lagrangian in the four-space [16] describes the charged particle motion in the electromagnetic field:

$$L(x^i,U^i;\tau)=-\frac{m}{2}U_iU^i-\frac{q}{c}U_iA^i, \tag{11}$$

where $x^i=(ct,x,y,z)$ is the four position vector, $U^i=dx^i/d\tau=(\gamma c,\gamma\vec{v})$ is the four-velocity, $d\tau=dt/\gamma$ is the proper time, $A^i=(\phi,\vec{A})$ is the electromagnetic field four-potential. The Einstein summation rule is used for repeating indices. The conjugate four-momentum is given by

$$P^i=-\frac{\partial L}{\partial U_i}=mU^i+\frac{q}{c}A^i,$$

and the corresponding Hamiltonian is also quadratic:

$$H(\tau)=P^iU_i+L=\frac{\left(P^i-\frac{q}{c}A^i\right)\left(P_i-\frac{q}{c}A_i\right)}{2m}. \tag{12}$$

Note that the value of the Hamiltonian, $H=\frac{1}{2}mc^2$, is invariant under Lorentz transformation. The covariant equations of motion are readily derived from this Hamiltonian:

$$\frac{dx^i}{d\tau}=\frac{\partial H}{\partial P_i}=\frac{P^i-\frac{q}{c}A^i}{m},$$

$$\frac{dP^i}{d\tau}=-\frac{\partial H}{\partial x_i}=\frac{P^k-\frac{q}{c}A^k}{m}\frac{q}{c}\frac{\partial A_k}{\partial x_i}.$$

It is worth pointing out that the space components of a covariant four-vector are equal to the negative 3D vector, e.g., $P_i=(P_0,-\vec{P})$, therefore, we can write the equations of motion for the space components, such as the x component and the time component, using an equivalent Hamiltonian $K=-H$,

$$\frac{dx}{d\tau}=\frac{\partial K}{\partial P_x},\quad \frac{dP_x}{d\tau}=-\frac{\partial K}{\partial x}\quad (i=1),$$

$$\frac{d(ct)}{d\tau}=\frac{\partial K}{\partial(-P_0)},\quad \frac{d(-P_0)}{d\tau}=-\frac{\partial K}{\partial(ct)}\quad (i=0).$$

Consequently, the equivalent Hamiltonian can be expressed in terms of conventional time and space quantities,

$$K(x,P_x,y,P_y,z,P_z,ct,-P_0;\tau)=\frac{\left(\vec{P}-\frac{q}{c}\vec{A}\right)^2-\left(P_0-\frac{q}{c}\phi\right)^2+m^2c^2}{2m}. \tag{13}$$

Note that by including the additional term $\frac{1}{2}mc^2$ in the above expression, the resultant Hamiltonian has a zero value. This particular feature of the Hamiltonian is critical for deriving a form of Hamiltonian using the real time t as an independent variable.

In the case of a static magnetic field, the scalar potential is zero and the vector potential is time independent. The total energy and momentum of the charged particle are constant, i.e., the relativistic parameter $\gamma=$const. As a result, the independent variable can be switched from the proper time τ to some scaled real time $\sigma=ct$ in the following manner:

$$d\tau\rightarrow d\sigma=c\gamma d\tau, K\rightarrow K/(c\gamma).$$

This yields an equivalent Hamiltonian with σ as an independent variable:

$$K(x,P_x,y,P_y,z,P_z,\bar{\tau},P_{\bar{\tau}};\sigma)=\frac{\left(\vec{P}-\frac{q}{c}\vec{A}\right)^2-P_{\bar{\tau}}^2+m^2c^2}{2mc\gamma},$$

where $\bar{\tau}=ct$ and $P_{\bar{\tau}}=-P_0=-\mathcal{E}/c=-\gamma mc$. The next step is to replace $mc\gamma$ in the denominator by $-P_{\bar{\tau}}$, which is permissible due to the zero value of the Hamiltonian,

$$K(x,P_x,y,P_y,z,P_z,\bar{\tau},P_{\bar{\tau}};\sigma)=-\frac{\left(\vec{P}-\frac{q}{c}\vec{A}\right)^2+m^2c^2}{2P_{\bar{\tau}}}+\frac{1}{2}P_{\bar{\tau}}.$$

The canonical momenta can be further scaled to yield the following equivalent Hamiltonian:

$$K(x,p_x,y,p_y,z,p_z,\bar{\tau},p_{\bar{\tau}};\sigma)=-\frac{(\vec{p}-\vec{a})^2+1/(\gamma_0^2\beta_0^2)}{2p_{\bar{\tau}}}+\frac{1}{2}p_{\bar{\tau}}, \tag{14}$$

where $\vec{a}$ and $\vec{p}$ have been defined in Eq. (3), $p_{\bar{\tau}}=P_{\bar{\tau}}/P_0$, $\beta_0=v_0/c$, and $\gamma_0=1/\sqrt{1-\beta_0^2}$ are relativistic parameters at the nominal energy.

Finally, to express the Hamiltonian in terms of momentum deviation and path length, the fourth canonical pair $(\bar{\tau},p_{\bar{\tau}})$ can be replaced by (δ,l). Using the relationship be-

tween δ and p_τ^-, $p_\tau^-=-\sqrt{(1+\delta)^2+1/(\gamma_0^2\beta_0^2)}$, a Hamiltonian depending on momentum deviation and path length can be derived:

$$K(x,p_x,y,p_y,z,p_z,\delta,l;\sigma)=\frac{(\vec{p}-\vec{a})^2-(1+\delta)^2}{2\sqrt{(1+\delta)^2+\dfrac{1}{\gamma_0^2\beta_0^2}}}. \tag{15}$$

With this quadratic form of the exact Hamiltonian, the technique outlined in Sec. IV can be readily applied to construct explicit symplectic integrators. It is important to note that this type of integrator uses the time integration in eight-dimensional (8D) phase space.

Finally, we would like to address the relationship between the time integration and space integration. In accelerators, magnetic devices and beam diagnostics are located along the beam direction. Likewise, many beam parameters are observed and measured along the beam line at a certain azimuthal position *s*. Therefore, it is convenient and logical to use *s* as the independent variable in the Hamiltonian [Eq. (3)]. Consequently, symplectic maps can be computed and symplectic tracking can be performed from one azimuthal location to another. However, to our knowledge no explicit integration method has been developed for the exact Hamiltonian with the square root using the space integration.

Using an alternative exact Hamiltonian for 3D magnetic fields, we have developed explicit integrators in 8D by resorting to the time integration. Direct time integration may be useful for a small circular accelerator in which the magnetic field is known globally. As an example, we have developed a FODO lattice consisting of a focusing quadrupole, a drift, a defocusing quadrupole, and another drift. Both quadrupoles in this FODO lattice possess extended fringe fields. The global magnetic field in the FODO lattice is the superposition of two quadrupole fields. Each of the quadrupole fields is represented by the following vector potential:

$$\vec{a}=(0,0,-\tfrac{1}{2}b(z)(x^2-y^2)),\quad b(z)=\frac{b_1}{\sqrt{2\pi}}\exp\left(-\frac{z^2}{2l_q^2}\right), \tag{16}$$

where b_1 and l_q are the focusing strength and effective length of the quadrupole, respectively. The fact that $\vec{\nabla}\times(\vec{\nabla}\times\vec{a})\neq 0$ does not change the nature of the problem, for it is equivalent to having an artificially introduced current source in the lattice. This additional term which allows the soft-edge modeling of the magnet is in fact physically and mathematically more correct than the hard-edge model which precludes going back to the original Hamiltonian. Numerically, we have confirmed that the second-order integrator for such a vector potential field is symplectic.

Knowing the exact global field for a storage ring with a large number of elements is practically impossible. In addition, the time-dependent tracking data are difficult to align for a particular *s* location for further analyses. These difficulties can be resolved by sticking to the space integration globally while providing a phase space conversion at the boundaries of those elements which need to be modeled by symplectic time integration. Such a conversion is topologically permissible if it occurs in the field-free region.

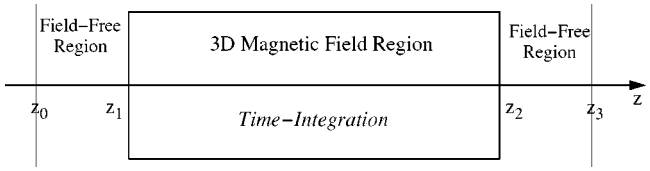

FIG. 1. Two steps are involved in symplectic integration from z_0 to z_3. Using the time integration for the exact Hamiltonian, the first step takes the particle from z_0 to a z location slightly passing z_2. In the field-free region, the second step takes the particle to the final position of z_3 using a canonical transformation.

This idea is illustrated in Fig. 1. Suppose that the 3D magnetic field can be practically confined between z_1 and z_2. To integrate from z_0 to z_3, the time integration can be first performed from z_0 to a z location slightly beyond z_2. In the field-free region between z_2 and z_3, the particle drifts forward to z_3 using the following Hamiltonian:

$$K_d(x,p_x,y,p_y,z,p_z,\delta,l;\sigma)=-\sqrt{(1+\delta)^2-p_x^2-p_y^2}+p_z.$$

Mathematically, the following canonical transformation is performed:

$$\Delta p_x=\Delta p_y=\Delta p_z=\Delta\delta=0,\quad \Delta\sigma=\Delta z,$$

$$\Delta x=\frac{p_x}{u}\Delta\sigma,\quad \Delta y=\frac{p_y}{u}\Delta\sigma,\quad \Delta l=\frac{1+\delta}{u}\Delta\sigma,$$

where $u=\sqrt{(1+\delta)^2-p_x^2-p_y^2}$, and Δz is the drift length. As a result of this practice, the local time integration is used to create a symplectic map between two locations in space, z_0 and z_3.

This localized time integration is tested with the same FODO lattice described above. The results are shown in Fig. 2. The symplectic condition of the tracking code is determined by the numerical behavior of the total momentum change in the drift space: $\delta p=(1+\delta)-\sqrt{p_x^2-p_y^2-p_z^2}$. The calculation shown in Fig. 2 is performed in the 8D phase space, always carrying the value of p_z during the tracking. We have found that δp would show no particular long-term trend of increasing or decreasing, therefore symplectic, if the following two conditions are met: (1) if the time integration is extended far enough from the quadrupole center (larger than $\pm 8l_q$); (2) if the number of integration steps is large enough ($\geqslant$50 steps). In this case, δp is small, of the order of 10^{-13}, and the change of p_z is also small in the last steps of integration. By meeting these conditions, the drift-forward operation is carried out in the field-free region in the numerical sense. Because p_z is frozen in the field-free region, the 8D symplectic dynamics is then reduced back to the 6D symplectic dynamics.

It is important to point out that when both horizontal and vertical motions are excited, particle's motion is coupled nonlinearly. Such nonlinear coupling is not present in the paraxial Hamiltonian. The nonlinear coupling in this FODO

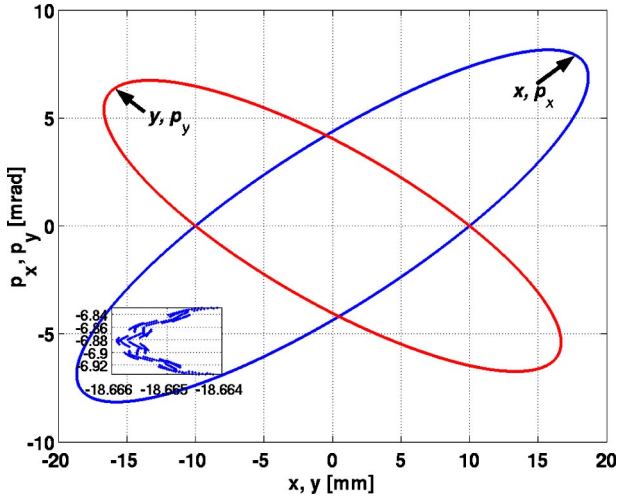

FIG. 2. A particle's phase space trajectories plotted at the end of a FODO lattice (QF for the focusing quadrupole and QD for the defocusing quadrupole). QF-DRIFT1-QD-DRIFT2 (100 000 turns). Quadrupole parameters are $(b_1)_{\mathrm{QF}}=6\ \mathrm{m}^{-2}$, $(b_1)_{\mathrm{QD}}=-5\ \mathrm{m}^{-2}$, $l_q=0.1$ m, and the fringe field extends to ± 1.0 m. The length of both drifts is $l_d=0.5$ m. Initially, the particle starts with $(x,p_x,y,p_y,\delta)=(0.01,0,0.01,0,0)$.

lattice is shown as finite thickness of the phase space ellipses and fast motion around the turning point in Fig. 2.

Clearly, the time integration for the exact Hamiltonian requires the development of proper 3D field models bounded by field-free regions. This remains a challenge for several reasons. First, the 3D field model should be analytic in the entire integration region. Second, to facilitate the conversion between the time and space integrations, the model should provide rapid tapering at the ends of the magnet. Third, if there is significant fringe field overlap from two adjacent magnets, they have to be treated as one magnetic device.

VI. A GENERAL WIGGLER INTEGRATOR FOR BEAM DYNAMICS STUDIES

To illustrate the usage of explicit symplectic integrators for 3D magnetic fields, we have developed a general symplectic tracking code for wigglers using the paraxial Hamiltonian of Eq. (4). The three-dimensional magnetic field for a horizontal planar wiggler can be described in the following form:

$$\frac{B_y}{B_0}=-\sum_{m,n} C_{mn}\cos(k_{xl}x)\cosh(k_{ym}y)\cos(k_{zn}z+\theta_n),$$

$$\frac{B_x}{B_0}=\sum_{m,n} \frac{C_{mn}k_{xl}}{k_{ym}}\sin(k_{xl}x)\sinh(k_{ym}y)\cos(k_{zn}z+\theta_n),$$

$$\frac{B_z}{B_0}=\sum_{m,n} \frac{C_{mn}k_{zn}}{k_{ym}}\cos(k_{xl}x)\sinh(k_{ym}y)\sin(k_{zn}z+\theta_n),$$

where B_0 is the amplitude of the peak magnetic field, C_{mn} are the relative amplitudes of wiggler harmonics, $k_{ym}^2=k_{xl}^2+k_{zn}^2$, $k_{zn}=nk_w$, $k_w=2\pi/\lambda_w$, λ_w is the wiggler period, and θ_n is the relative phase of the nth wiggler harmonic. The wiggler harmonic expansion of the magnetic field allows the modeling of realistic wiggler fields. For example, a next linear collider (NLC) damping ring wiggler with saturated pole tips can be modeled with a few tens of wiggler harmonics to achieve 10^{-3} or better relative field accuracy [17].

Before this work, explicit symplectic integrators based on a simple average Hamiltonian method of Smith [18] or similar techniques had been used for wiggler tracking [17,19–21]. By retaining the most important nonlinear term in the system, this method is rather efficient. However, the accuracy of the tracking results needs to be verified with a direct wiggler integrator described in the following.

By choosing $A_z=0$, a more efficient integrator is obtained with the vector potential: $\vec{A}=(A_x,A_y,0)$. The scaled vector potential $\vec{a}=q\vec{A}/P_0c$ is given by

$$a_x=\sum_{m,n} D_{mn}\cos(k_{xl}x)\cosh(k_{ym}y)\sin(k_{zn}z+\theta_n),$$

$$a_y=\sum_{m,n} D_{mn}\frac{k_{xl}}{k_{ym}}\sin(k_{xl}x)\sinh(k_{ym}y)\sin(k_{zn}z+\theta_n),$$

$$a_z=0, \tag{17}$$

where $q=-|e|$ for electrons, $D_{mn}=C_{mn}(K/\gamma_0\beta_0)\times(k_w/k_{zn})$, $K=eB_0/mc^2k_w$ is the wiggler parameter, and γ_0, β_0 are the relativistic parameters at the nominal energy. For vertical planar wigglers, similar harmonic expressions for fields can be obtained by changing x to y and y to $-x$ in the above expressions [22].

The magnetic field for an arbitrarily polarized wiggler can be expressed as a superposition of a horizontal wiggler and vertical wiggler field. This allows us to develop a general wiggler tracking code using wiggler harmonics. This tracking code has been implemented in several tracking codes including TRACY [23] and AT [24].

Symplectic wiggler tracking has been used to study Duke FEL storage ring beam dynamics. The Duke FEL storage ring is a dedicated FEL light source with a small emittance ($\epsilon_x=18$ nm rad at 1 GeV). Like third-generation light sources with a small emittance, the ring performance is critically dependent on the dynamic aperture [20,21]. Unlike many conventional light source rings, the Duke ring is designed with long straight sections to maximize space for FEL wigglers. Accurate dynamics studies with long FEL wigglers become possible with the above generic wiggler tracking code. Our studies also use the frequency map analysis technique of Laskar [25–27] to gain in-depth understanding about the particle's loss mechanism.

In the Duke ring, the present FEL consists of two electromagnetic OK4 wigglers, each 3.4 m long separated by a three-pole buncher magnet (see Table I). The main field of the OK4 wigglers can be described by the fundamental harmonic with its B_y component as $B_y=-B_0\cosh(k_wy)\cos(k_wz)$. The wiggler tracking is somewhat optimized for efficiency by using a second-order integrator and five integration steps per wiggler period.

The significance of dynamics impact of the OK4 wigglers is illustrated by the change in dynamic aperture after the wigglers are turned on. Figure 3 shows the on-momentum

TABLE I. The OK-4 wiggler parameters.

	OK-4 FEL
Total wiggler length (m)	6.7
Number of wigglers	2
Number of periods per wiggler	33.5
Wiggler periods (cm)	10
Wiggler gap (mm)	22
Peak magnetic field (kG)	5.5
Max. wiggler $K=\frac{eB_0}{k_w m_e c^2}$	5.1

dynamic aperture of the Duke ring with OK4 wigglers turned off. A number of excited resonances are identified and labeled in both the configuration plot and tune plot. In the x direction, the dynamic aperture is limited by the sixth-order resonance (i) with $6\nu_x=55$. The horizontal loss region is connected to the high diffusion region at some vertical amplitudes as a result of two-resonance overlap: (d) with $2\nu_x+4\nu_y=35$ and (e) with $7\nu_x=64$. In the y direction, the loss region around the resonance (g) with $3\nu_x+4\nu_y=44$ provides a practical limitation for the vertical aperture. Beyond it, the typical third-order sextupole resonance (h) with $\nu_x-2\nu_y=1$ is excited, forming a triangular island. It is interesting to observe that at even higher vertical amplitude there exists a stable region which corresponds to a cross point in the tune space at $(\nu_x,\nu_y)=(9.25,4.125)$. However, the stable region beyond the resonance (g) is washed out when various lattice errors are taken into account.

Figure 4 shows the dynamic aperture with OK4 wigglers turned on. Compared with the wiggler-off case, the most apparent difference is the tune space footprint. The horizontal tune spread is roughly the same (from 9.11 to 9.20). However, while decreasing from 4.186 to 4.12 with wigglers off, the vertical tune spread with amplitude increases from 4.186 to 4.22 with wigglers on. This is the result of the strong nonlinear wiggler focusing. Because of a different tune spread footprint, different parts of the tune space are being sampled by particles when wigglers are turned on, which in turn excites different resonances. For example, both figures show a four-resonance crossing at about the same horizontal amplitude of 10 mm, but with different vertical amplitudes. Like the case with the wiggler off, the horizontal aperture is limited by the same sixth-order resonance. In the vertical direction, the situation is rather different. With the wiggler on, the vertical aperture is not limited by any resonances. Instead, it shows an almost sudden transition from an intermediate level of diffusion to a complete particle loss. This effect can be attributed to the exponential increase of the wiggler field near the vertical pole tips as expressed in the hyperbolic functions. In such a case, the wiggler field acts like a kind of hard limit for the vertical aperture. As a result, the vertical aperture is somewhat reduced to 13.6 mm.

We have also studied the dynamics impact of circularly polarized FEL wigglers in the Duke ring. In particular, the off-momentum dynamic aperture has been computed to determine the available dynamic momentum aperture for various wiggler and storage ring operation conditions [28].

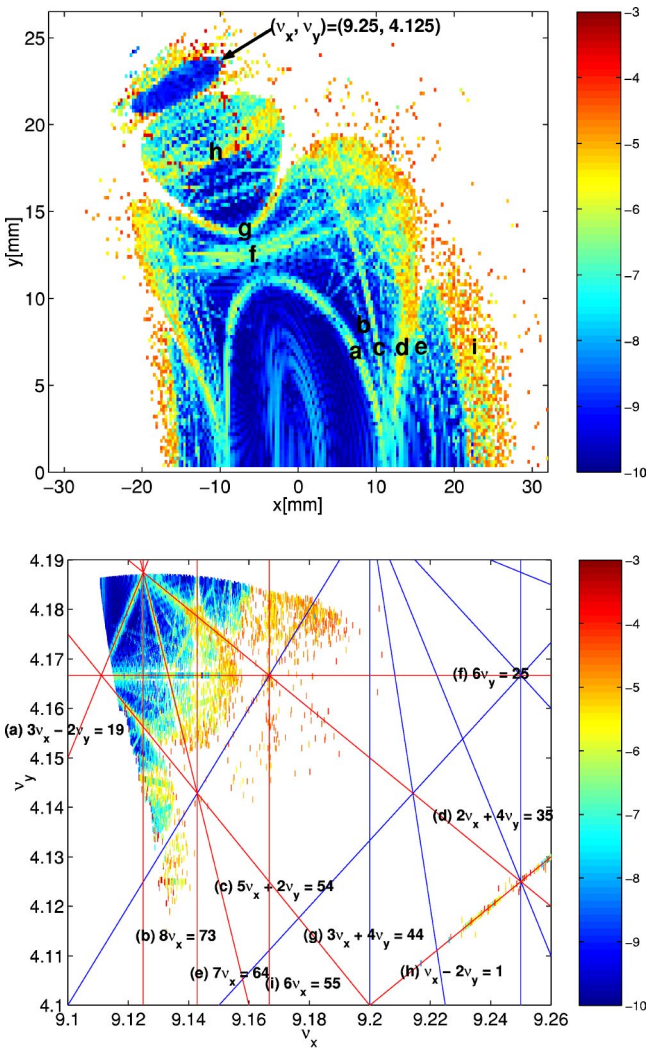

FIG. 3. (Color online) On-momentum dynamic aperture of Duke storage ring at the center of the arc with $\beta_x=2.48$ m, $\beta_y=1.57$ m. The OK4 wigglers are turned off, the nominal energy is 1 GeV, and the number of tracking turns is 1000. The shaded areas in plots indicate different diffusion rates. Unplotted white spaces are regions where particles are lost during tracking. (For colored online figures, the diffusion rate per turn is computed in a logarithmic scale and then mapped to a color map: blue areas indicate low diffusion regions, red areas indicated high diffusion region). Various excited resonance lines [from (a) to (h)] are identified and labeled in the frequency map plot (the lower plot) and in the configuration space plot (the upper plot).

VII. CONCLUDING REMARKS

Although Ruth first speculated in 1980s [1] that an explicit high-order map might be possible for a Hamiltonian of the form $H=[\vec{p}-\vec{a}(\vec{q},t)]^2/2$, the exact procedure to construct such a high-order symplectic integrator was not developed until this work. Furthermore, we have successfully developed a quadratic Hamiltonian for the exact particle

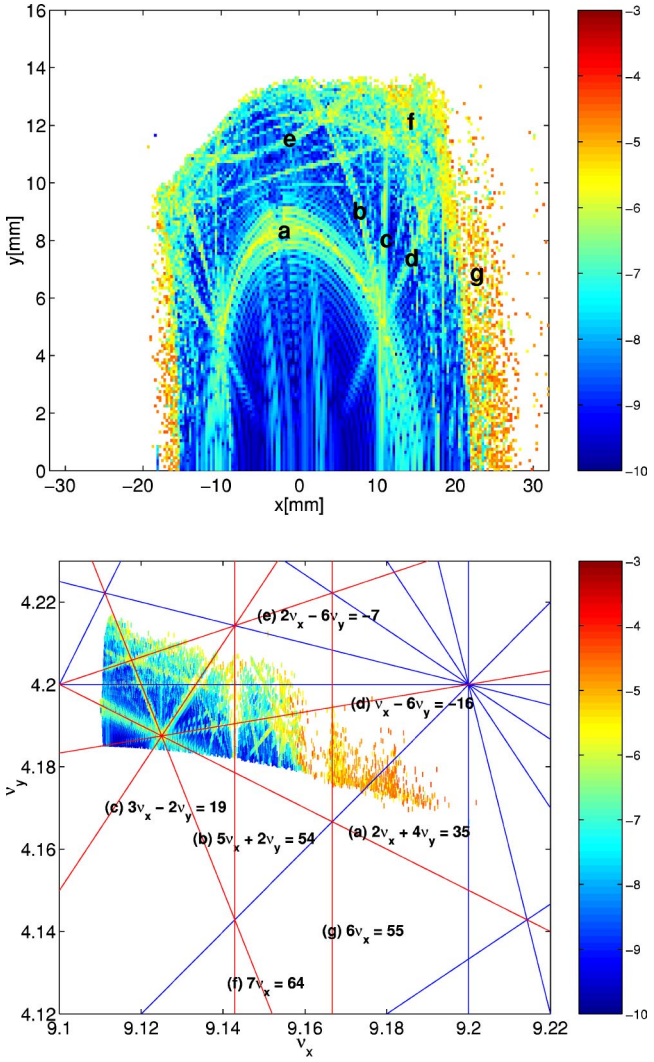

FIG. 4. (Color online) On-momentum dynamic aperture of Duke storage ring at the center of the arc with $\beta_x = 2.48$ m, $\beta_y = 1.57$ m. The OK4 wigglers are turned on with a wiggler $K = 5.1$, the nominal energy is 1 GeV, and the number of tracking turns is 1000. The description of the shaded area (color map) is the same as for the previous figure.

motion in the static 3D magnetic field. Via the time integration, this Hamiltonian has allowed the development of explicit symplectic integrators for any 3D magnetic elements in accelerators without paraxial approximation.

Explicit symplectic integrators for *s*-dependent magnetic fields are essential for understanding single-particle beam dynamics in the next generation storage rings, from light source rings to linear collider damping rings to the Neutrino Factory and Muon Collider. Two types of applications are particularly important. The first type is the modeling of the magnet fringe field. For example, superconducting dipoles and wavelength shifters are increasingly becoming a preferred radiation source for hard x rays in some third-generation light source rings. The *s*-dependent magnetic field in such devices can be properly modeled using an explicit symplectic integrator described in this paper.

The second type of application is the modeling of magnetic undulators and wigglers with linear, circular, or arbitrary polarizations. Before this work, explicit symplectic integrators had resorted to the average Hamiltonian (Sec. VI). In addition, implicit methods based upon generation functions, both analytical and numerical, had been developed [29–31]. While very useful, these methods have various limitations and their accuracy needs to be benchmarked with the direct symplectic wiggler integration method presented in this paper. This method allows direct trajectory tracking in wigglers in the same way as for magnetic multipoles. The usefulness of this technique has been demonstrated by our study of the Duke storage ring dynamics with the OK4 FEL wigglers (Sec. VI).

Finally, we would like to comment on the time integration for exact Hamiltonian and its use in existing 6D tracking codes. First, it remains a challenge to model the 3D magnetic field using an analytic representation with a rapid tapering. Second, as demonstrated in the FODO lattice example (Sec. V), reducing 8D symplectic dynamics to the 6D symplectic dynamics can be done in the field-free region. However, a careful study has yet to be performed to determine if the variable p_z need be carried around for the part of tracking performed in 6D tracking codes.

ACKNOWLEDGMENTS

The authors would like to thank J. Laskar at Astronomie et Systèmes Dynamiques for his frequency analysis package NAFF and C. Steier at LBNL for sharing with us the frequency map visualization techniques. One of the authors (Y.K.W.) would also like to thank V. Litvinenko at Duke University and B. Kincaid at LBNL for encouragement and support. Work of Y.K.W. was supported by U.S. Department of Energy Grant No. DE-FG05-91ER40665. Work of D.S.R. was supported by the Director, Office of Energy Research, Office of Basic Energy Sciences, Material Sciences Division, U.S. Department of Energy, under Contract No. DE-AC03-76SF00098.

[1] R.D. Ruth, IEEE Trans. Nucl. Sci. **30**, 2669 (1983).
[2] F. Neri, Lie algebras and canonical integration, Department of Physics Technical Report, Univeristy of Maryland, 1988 (unpublished).
[3] E. Forest and R.D. Ruth, Physica D **43**, 105 (1990).
[4] H. Yoshida, Phys. Lett. A **150**, 262 (1990).
[5] E. Forest, J. Bengtsson, and M.F. Reusch, Phys. Lett. A **158**, 99 (1991).
[6] E. Forest, *Beam Dynamics–A New Attitude and Framework* (Harwood Academic, Chur, Switzerland, 1998).
[7] W. Wan *et al.*, Nucl. Instrum. Methods Phys. Res. A **427**, 74 (1999).
[8] M. Berz, B. Erdelyi, and K. Makino, Phys. Rev. ST Accel. Beams **3**, 124001 (2000).

[9] D. Abell, F. McIntosh, and F. Schmidt, Phys. Rev. ST Accel. Beams, **6**, 064001 (2003).
[10] L. Schachinger and R. Tolman, Part. Accel. **22**, 35 (1987).
[11] E. Forest, KEK, PTC, the polymorphic tracking code (2002), a wiggler integrator is developed in Collaboration with D. Sagan at Cornell as a module for BMAD.
[12] R. McLachlan and G.R.W. Quispel, *Foundations of Computational Mathematics*, edited by R. DeVore, A. Iserles, and E. Suli (Cambridge University Press, Cambridge, 2001), pp. 155–210.
[13] See http://www.math.ntnu.no/num/synode
[14] R. McLachlan, BIT Numerical Mathematics **35**, 258 (2003).
[15] L. Nadolski and J. Laskar, in *Proceedings of the European Particle Accelerator Conference, 2002* (EPS-IGA and CERN, Geneva, 2002), p. 1276–1278.
[16] J.D. Jackson, *Classical Electrodynamics*, 3rd ed. (Wiley, New York, 1998).
[17] A. Wolski and Y. Wu, in *Proceedings of the 2001 Particle Accelerator Conference* (IEEE, Piscataway, NJ, 2001), pp. 3798–3800.
[18] L. Smith, LBNL Report, No. LBL-21391, 1986 (unpublished).
[19] P. Elleaume, in *Proceedings of the European Particle Accelerator Conference, Berlin* (Editions Frontieres, Gif-sur-Yvette, 1992), p. 661.
[20] Y. Wu, V.N. Litvinenko, E. Forest, and J.M.J. Madey, Nucl. Instrum. Methods Phys. Res. A **331**, 287 (1993).
[21] Y. Wu, V.N. Litvinenko, and J.M.J. Madey, Nucl. Instrum. Methods Phys. Res. A **341**, 363 (1994).
[22] Y.K. Wu *et al.*, in *Proceedings of the 2001 Particle Accelerator Conference* (IEEE, Piscataway, NJ, 2001), pp. 459–461.
[23] H. Nishimura and J. Bengtsson (private communication).
[24] A. Terebilo, in *Proceedings of the 2001 Particle Accelerator Conference* (IEEE, Piscataway, NJ, 2001), p. 3202–3205.
[25] J. Laskar, Icarus **88**, 266 (1990).
[26] J. Laskar, Physica D **67**, 257 (1993).
[27] D. Robin, C. Steier, J. Laskar, and L. Nadolski, Phys. Rev. Lett. **85**, 558 (2000).
[28] Y.K. Wu, J. Li, S.F. Mikhailov, and V.N. Litvinenko, in Proceedings of the 2003 Particle Accelerator Conference (unpublished).
[29] J. Bahrdt and G. Wustefeld, Techinical Reports, Bessy TR No. 158 (1990) and Bessy TR No. 163 (1991) (unpublished).
[30] M. Scheer and G. Wustefeld Technical Report, Bessy TR No. 169 (1992) (unpublished).
[31] M. Scheer and G. Wustefeld, Proceedings of the 1997 Particle Accelerator Conference (unpublished), Vol. 2, p. 2606.